

Draft Genomes of *Amaranthus tuberculatus*, *Amaranthus hybridus*, and *Amaranthus palmeri*

Jacob S. Montgomery¹, Darci Giacomini¹, Bridgit Waithaka², Christa Lanz², Brent P. Murphy¹, Ruth Campe³, Jens Lerchl³, Andreas Landes³, Fanny Gatzmann⁴, Antoine Janssen⁵, Rudie Antonise⁵, Eric Patterson ⁶, Detlef Weigel², and Patrick J. Tranel ^{1,*}

¹Department of Crop Sciences, University of Illinois, Urbana

²Max Planck Institute for Developmental Biology, Tübingen, Germany

³BASF SE, Limburgerhof, Germany

⁴BASF SE, Ludwigshafen, Germany

⁵Keygene N.V., Wageningen, The Netherlands

⁶Department of Plant, Soil and Microbial Sciences, Michigan State University

*Corresponding author: E-mail: tranel@illinois.edu.

Accepted: 15 August 2020

Data deposition: This project has been deposited at CoGe at <https://genomeevolution.org/coge/> under accessions 56882, 56678, 57896, 57427, 57429, and 55760; and with the National Center for Biotechnology Information under accessions PRJNA641102, PRJNA640356, and PRJNA655730.

Abstract

Amaranthus tuberculatus, *Amaranthus hybridus*, and *Amaranthus palmeri* are agronomically important weed species. Here, we present the most contiguous draft assemblies of these three species to date. We utilized a combination of Pacific Biosciences long-read sequencing and chromatin contact mapping information to assemble and order sequences of *A. palmeri* to near-chromosome-level resolution, with scaffold N50 of 20.1 Mb. To resolve the issues of heterozygosity and coassembly of alleles in diploid species, we adapted the trio binning approach to produce haplotype assemblies of *A. tuberculatus* and *A. hybridus*. This approach resulted in an improved assembly of *A. tuberculatus*, and the first genome assembly for *A. hybridus*, with contig N50s of 2.58 and 2.26 Mb, respectively. Species-specific transcriptomes and information from related species were used to predict transcripts within each assembly. Syntenic comparisons of these species and *Amaranthus hypochondriacus* identified sites of genomic rearrangement, including duplication and translocation, whereas genetic map construction within *A. tuberculatus* highlighted the need for further ordering of the *A. hybridus* and *A. tuberculatus* contigs. These multiple reference genomes will accelerate genomic studies in these species to further our understanding of weedy evolution within *Amaranthus*.

Key words: *Amaranthus*, genome evolution, trio binning, chromatin contact mapping, linkage mapping, weed genomics.

Significance

The production of reference genome assemblies has accelerated the study of basic biology and evolution within many species, but these resources have yet to be developed for many agronomically important weeds. This work reports new or improved genomes for three such weed species that will allow for the study of many biological questions.

Introduction

The genus *Amaranthus* contains some of the most agronomically important weeds, including *Amaranthus tuberculatus* (Moq.) J.D. Sauer, *Amaranthus hybridus* L., and *Amaranthus palmeri* (S.) Watson (Sauer 1957, 1967). The ability of these *Amaranthus* species to evolve herbicide resistance via de novo mutation or interspecific hybridization makes them primary targets of weed management programs (Culpepper et al. 2006; Tranel et al. 2011; Gaines et al. 2012). The availability of high-quality reference genomes in *Amaranthus* species would allow for more robust genomic and molecular studies within these species including elucidating the evolution of weedy traits such as herbicide resistance, which are often the result of very strong selection pressures exerted across vast geographic distances and under many different environments (Korte and Farlow 2013; Patterson et al. 2019). These selection pressures afford a unique opportunity to explore evolution and ecology under extraordinary conditions. Furthermore, the creation of such resources would contribute to an international effort to develop tools for the study of genomics in the world's worst weeds (Tranel and Trucco 2009; Ravet et al. 2018).

To date, some work on *Amaranthus* genomes has been published. Lightfoot et al. (2017) previously utilized Pacific Biosciences (PacBio) sequencing and Hi-C chromosome contact mapping to assemble and order the genome of *Amaranthus hypochondriacus*, an emerging pseudocereal crop species. Additionally, Kreiner et al. (2019) and Molin et al. (2020) reported the first genome assemblies of *A. tuberculatus* and *A. palmeri*, respectively.

In this work, we report the most contiguous draft assemblies of *A. tuberculatus*, *A. hybridus*, and *A. palmeri* to date. First, we produced haploid assemblies of *A. tuberculatus* and *A. hybridus* using the trio binning technique (Koren et al. 2018), which limited confounding effects from heterozygosity and avoided coassembly of alleles. This approach included generating PacBio sequences of an interspecific hybrid of *A. tuberculatus* and *A. hybridus*. Using short-read sequence data from each parent, the PacBio reads of this hybrid were binned based on short subsequences unique to each parental genome. The two resulting groups of PacBio reads were then assembled separately. Second, we assembled and ordered the *A. palmeri* genome into near-chromosome-level scaffolds using PacBio sequencing and Hi-C chromosome contact mapping. All assemblies were passed through repeat-masking and annotation pipelines. We conclude with a brief discussion of genome structure and synteny among *Amaranthus* species, obtained by comparing the newly produced genomes with the chromosomal organization of a closely related species, *A. hypochondriacus*. Synteny analysis included a version of the *A. tuberculatus* genome scaffolded based on recombination frequencies derived from segregating F_2 populations, which identified chromosomal rearrangement not detected

by anchoring the contigs to the pseudochromosomes of *A. hypochondriacus*.

Materials and Methods

Trio-Binned Genome Assemblies

Hybrid Development and Identification

An interspecific cross was made between a male *A. tuberculatus* plant of the ACR population, a population with dominant resistance to the herbicide imazethapyr (Patzoldt et al. 2005; Patzoldt and Tranel 2007), and an herbicide-sensitive *A. hybridus* plant. To identify interspecific hybrids, seed produced from this cross was scattered over moistened soil, treated with 1,066 g ae ha⁻¹ of imazethapyr (Pursuit herbicide, BASF, Ludwigshafen, Germany), covered with a thin layer of soil, and watered regularly. Each survivor was tested with primer set MU_657.2 under conditions described by Montgomery et al. (2019) to confirm hybrid identity and identify male hybrids.

Parental Sequencing

Genomic DNA was extracted from the two parents of the cross between *A. tuberculatus* and *A. hybridus* according to a described protocol (Xin and Chen 2012) and used to generate short-read sequencing libraries. These libraries were then sequenced to a coverage of ~100× on a HISEQ 3000 instrument (Illumina, San Diego, CA) using a HISEQ3000/4000 SBS kit and a paired-end 150 base read chemistry.

Hybrid Sequencing

High-molecular weight genomic DNA was extracted from an identified hybrid and used to create SMRTbell templates, which were sequenced on a Sequel II system (Pacific Biosciences, Menlo Park, CA).

Haplotype Assembly and Polishing

About 116.8 Gb of Sequel II long-read data were trio binned using the trio bin feature of *Canu*, and the two haplotypes were subsequently assembled using *Canu* (version 1.8; correctedErrorRate=0.04 corMhapSensitivity=normal genomeSize=XXX corMhapFilterThreshold=0.000000002 corMhapOptions="--threshold 0.80 --num-hashes 512 --num-min-matches 3 --ordered-sketch-size 1,000 --ordered-kmer-size 14 --min-olap-length 2000 --repeat-idf-scale 50" mhapBlockSize=500 ovlMerDistinct=0.975; Koren et al. 2017). The parameter genomeSize was set to 700 and 500 m for assembly of *A. tuberculatus* and *A. hybridus*, respectively. The binned subreads from each species were aligned to their respective assemblies using *Minimap2* (version 2.17; --sort, other parameters default; Li 2018). This alignment was used to polish the raw contigs with *Arrow* (*pbgccpp*,

version 1.9.0). Both assemblies were also finished against the *A. hypochondriacus* genome (Lightfoot et al. 2017) using *REVEAL finish* (commit 98d3ad1; Kreiner et al. 2019). Depth of coverage was calculated using *samtools depth* and *Minimap2* alignments (version 1.7; Li et al. 2009), and plotted in R (R Core Team 2018).

Haplotype Assembly Annotation

Parallel methodologies were used to repeat-mask and annotate the *A. tuberculatus* and *A. hybridus* genomes in *GenSaS* (version 6.0; Humann et al. 2019). In each species, a library of predicted repeats, generated with *RepeatModeler* (version 1.0.11; www.repeatmasker.org), was combined with a library of repeats identified using *RepeatMasker* (version 4.0.7; Smit et al. 2013) and an *Arabidopsis thaliana* repeat library within *GenSaS* to create a consensus library of repeats and mask each polished assembly. Nucleotide and protein sequence of *A. tuberculatus*, *A. palmeri*, *A. hypochondriacus* reference transcriptomes (Riggins et al. 2010; Giacomini D, unpublished data; Lightfoot et al. 2017) were aligned to each assembly using BlastN (version 2.7.1; Camacho et al. 2009) and BlastX (version 2.6.0; Camacho et al. 2009), respectively. These alignments were combined with results of gene prediction modeling (*AUGUSTUS*; version 3.1.1; Stanke et al. 2004) to generate an official gene set and identify predicted transcripts within each masked assembly (EVIDENCEModeler, release June 25, 2012, Haas et al. 2008). Predicted transcripts were prescribed function based on alignment (BlastP; version 2.2.28, -evaluate 1e-6 -max_hsps_per_subject 1 -max_target_seqs 1; Camacho et al. 2009) to the UniProtKB database.

Genetic Map Construction of *A. tuberculatus*

Two pseudo-F₂ mapping *A. tuberculatus* populations, POP1 and POP2, were established from single plant crosses, in which the same male *A. tuberculatus* plant was used for both crosses. Whole-genome sequence was generated for each parent using a Hi-Seq 4000 instrument, yielding 150-bp paired-end reads. Double-digest restriction-site associated DNA sequencing libraries were generated following Montgomery et al. (2019) for 285 individuals randomly selected from each population. Libraries were sequenced using a NovaSeq S1 flowcell (Illumina, San Diego, CA). Variant calling was conducted following the GATK 4.0 pipeline following best practices recommendations with variants hard filtered (FS>20, MQ<50, MQRankSum<-2, -3 < ReadPosRank Sum<4, SOR>4, QD<10; Poplin et al. 2017). The filtering pipeline *filter_variants_mapping.sh* was implemented to obtain mapping quality variants and is available through GitHub ([brentpm2/genetic_map_tuberculatus](https://github.com/brentpm2/genetic_map_tuberculatus)). Retained variants were observed in parent and at least 10% of pseudo-F₂ individuals. Contigs with two or more variants were retained within 100 individuals per population, and missing data

imputed with *Beagle* (version 4.0, Browning and Browning 2007). Variants that deviated from the expected 1:2:1 segregation ratio were removed. A genetic map was constructed with R/qtl independently for each population, where marker order on each contig was retained during analysis, and contig order was compared (Broman et al. 2003).

Amaranthus palmeri Genome Assembly

Several *A. palmeri* populations were passed through a previously described sequence-based genotyping pipeline (Truong et al. 2012) to quantify the level of heterogeneity and heterozygosity present within each population and plant, respectively. The population LIH06329 showed a dense cluster in a principal component analysis formed by individual plants, indicating low heterogeneity. Additionally, plants from this population showed sensitivity to multiple herbicides tested from eight herbicide modes-of-action classes 2, 4, 5, 6, 9, 10, 14, and 27 (see <https://hracglobal.com/tools/hrac-mode-of-action-classification-2020-map>; last accessed September 2, 2020). The 30 representative plants from LIH06329 had an average heterozygosity measure of 26.8% based on sequence information at 5556 loci generated through the sequence-based genotyping pipeline mentioned above. Leaf material from the plant with the lowest heterozygosity measure (21.2%) was harvested and used for sequencing.

Part of this material was sent to Dovetail (Scotts Valley, CA) to prepare and sequence Hi-C (211 M read pairs; 150 bp) and Chicago (235 M read pairs; 150 bp) libraries for chromosome scale scaffolding. High-molecular weight genomic DNA was extracted from the remaining leaf material. This DNA was used to generate ~20-kb insert size selected PacBio Sequel I libraries, which were sequenced using DNA 2.1 Polymerase chemistry.

About 106 Gb of long-read data were used to produce a de novo genome assembly using HGAP 5.1 (Chin et al. 2013). Raw reads were used to polish the resulting contigs as described above using *Arrow* (SMRTlink version 5.1.0). The polished assembly was provided to Dovetail to perform chromosome scale scaffolding based on chromatin contact mapping data generated through a Hi-C approach using the HiRise method (Putnam et al. 2016) and further improved by gap-filling using PBJelly (English et al. 2012). Regions of high heterozygosity that were falsely separated in this haploid assembly were purged using Haplomerger2 (filter_score2 = 500k, minOverlap = 10k; Huang et al. 2017). These scaffolds were passed through a repeat-masking and annotation pipeline analogous to the one described above for *A. tuberculatus* and *A. hybridus*.

Interspecific Synteny Comparison

To identify differences in genomic structure and detect regions of synteny between the species described above, *A. palmeri* scaffolds, polished contigs of *A. tuberculatus* and

Table 1Summary Statistics of *Amaranthus palmeri*, *Amaranthus tuberculatus*, and *Amaranthus hybridus* Draft Genome Assemblies

	<i>A. palmeri</i>	<i>A. tuberculatus</i>	<i>A. tuberculatus</i> (Kreiner et al. 2019)	<i>A. hybridus</i>
Estimated genome size (n, Mb) ^a	421.8	675.6	675.6	503.8
Assembly size (Mb)	408.1	572.9	663.7	403.0
Number of contigs	638	841	2,514	640
Number of scaffolds	303	16 ^b	16 ^b	16 ^b
Contig N50 length (Mb)	2.54	2.58	1.74	2.26
Scaffold N50 length (Mb)	20.11	34.7 ^b	43.1 ^b	24.5 ^b
Annotated genes	29,758	26,784	56,936	24,325
Complete BUSCO	84.2%	81.9%	88%	89.8%

^aGenome size estimates from cytological studies by Stetter and Schmid (2017).^bScaffolded with respect to *Amaranthus hypochondriacus* pseudochromosomes (Lightfoot et al. 2017).

A. hybridus, and *A. tuberculatus* scaffolds produced using the genetic map were each compared with the 16 pseudo-chromosomes of the *A. hypochondriacus* genome (Lightfoot et al. 2017) using Synmap2 (Legacy Version=True, Syntenic Path Assembly=True; Haug-Baltzell et al. 2017). The genome of *A. hypochondriacus* was also compared with itself to visualize endogenous duplications across the genome.

Results and Discussion

The trio binning technique successfully isolated sequence from each haplotype of the *A. tuberculatus*×*A. hybridus* hybrid. Of 116.8-Gb PacBio subread sequence produced, 35.3% was binned as *A. hybridus*, 64.4% as *A. tuberculatus*, and only 0.1% as ambiguous, with the remaining 0.2% removed because reads containing this sequence were shorter than 1 kb. The higher proportion of sequences belonging to the *A. tuberculatus* haplotype is partially explained by differences in genome size: haploid genome sizes previously were estimated to be 675 and 503 Mb for *A. tuberculatus* and *A. hybridus*, respectively (Stetter and Schmid 2017).

Independent assembly of each bin resulted in the first reported *A. hybridus* reference genome assembly and a more contiguous assembly than the previously reported *A. tuberculatus* reference (Kreiner et al. 2019; table 1). Discrepancies between estimated and assembled genome size in these two species are likely due to the lack of centromeric and telomeric regions in our assemblies (Lamb and Birchler 2003; Kim et al. 2019). Additionally, because only one haplotype was included in the assembly process, we are confident that multiple alleles do not inflate our assembly size. This conclusion is supported by the presence of only one peak in the distributions of coverage across these assemblies, circumventing the need for additional finishing steps, such as haplotype merging (supplementary fig. S1, Supplementary

Material online). By anchoring each of these genomes against the reference *A. hypochondriacus* assembly, we placed 99.6% of the *A. tuberculatus* and 99.8% of the *A. hybridus* assemblies onto the 16 pseudo-chromosomes of the *A. hypochondriacus* assembly. Our assembly of a male *A. tuberculatus* individual complements the previous assembly of a female (Kreiner et al. 2019), allowing for future comparative studies that may elucidate the genetic basis of dioecy in this species. The success of trio binning to produce *A. tuberculatus* and *A. hybridus* genome assemblies sets a precedent for this technique to be used in other plant species that produce viable interspecific hybrid progeny, such as *Ambrosia trifida* and *Ambrosia artemisiifolia* (Vincent and Cappadocia 1987).

The linkage maps generated for POP1 and POP2 from *A. tuberculatus* agreed in contig order (supplementary table S1 and fig. S2, Supplementary Material online). As a shared parent is observed in each population, this suggests the lax variant filtration was still reflective of the overall genome structure. The map of POP1 was more complete than POP2, representing 74% of the total genomic sequence across 16 linkage groups. Although not sufficient for the complete scaffolding of the *A. tuberculatus* genome, the map allowed for a better comparison of synteny between *A. tuberculatus* and *A. hypochondriacus* (discussed below).

Our genome assembly pipeline for *A. palmeri* resulted in a highly contiguous reference genome with some chromosomes seemingly being assembled from end-to-end (table 1 and fig. 1). Recombination frequency across the genome could be derived from future linkage studies to validate the order of these contigs and further develop this genomic resource. These results confirm the efficacy of this “PacBio-plus-Hi-C” genome assembly approach, even in species known to be highly heterozygous (Laforest et al. 2020).

To identify structural differences in each species' genome, syntenic comparisons between each assembly and the 16 pseudo-chromosomes of *A. hypochondriacus* were made

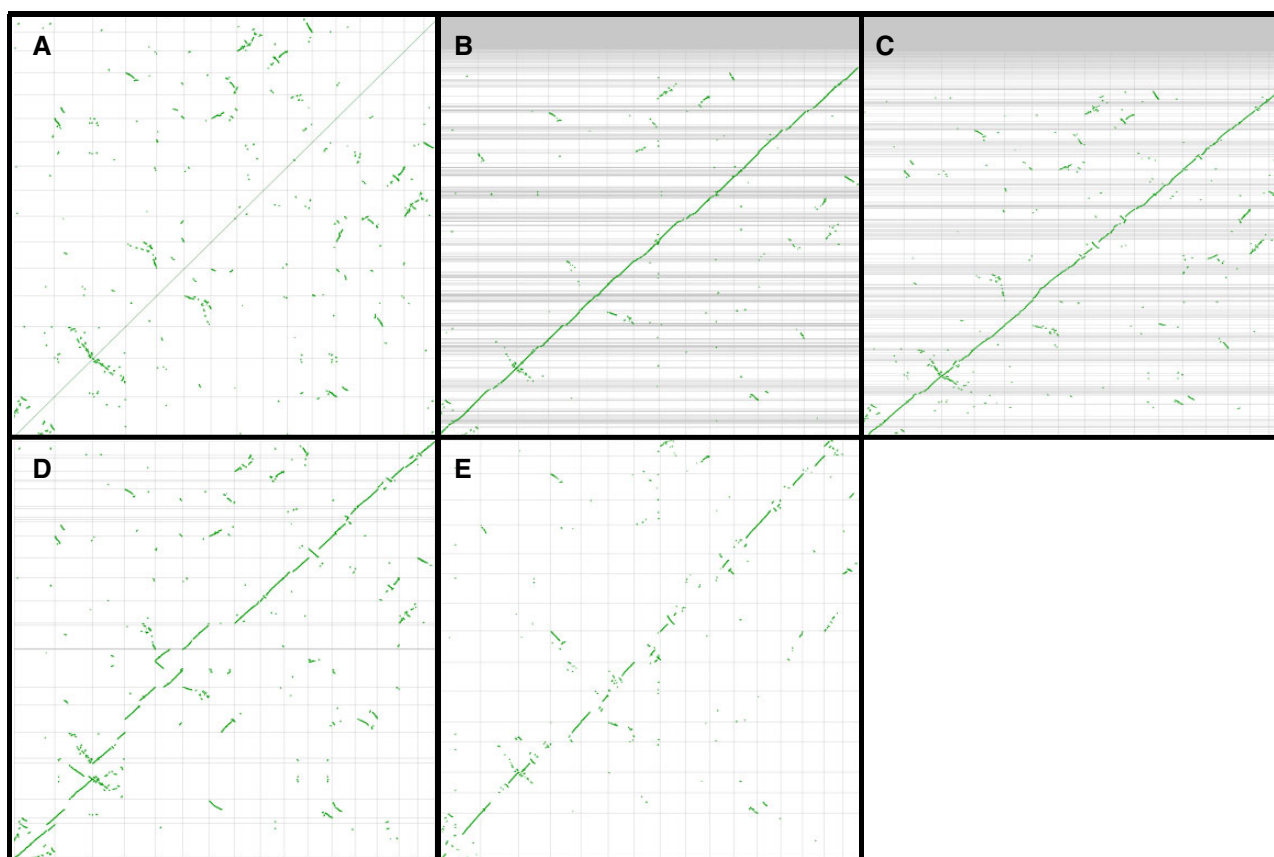


Fig. 1.—Dot plots demonstrating synteny between the genome of *Amaranthus hypochondriacus* and itself (A), the contigs of *Amaranthus hybridus* (B), and *Amaranthus tuberculatus* (C) as well as the scaffolds of *Amaranthus palmeri* (D). Panel (E) is an analogous plot comparing the *A. tuberculatus* contigs arranged according to linkage map generated from POP1 and the scaffolds of *A. hypochondriacus*. Within each panel, the 16 pseudochromosomes of *A. hypochondriacus* are represented along the X axis, separated by vertical lines. The contigs/scaffolds of genome assemblies from each other species are represented along the Y axis of their respective panes, separated by horizontal lines. Each green dot represents one syntenic gene, and obvious diagonals indicate syntenic regions between the two compared species.

with Synmap2 (fig. 1). No major differences in chromosome structure were identified between *A. hypochondriacus* and *A. hybridus*, which was expected, as recent phylogenetic studies suggest these two species to be very closely related (Waselkov et al. 2018). Several small-scale inverted regions were detected within the contigs of the *A. tuberculatus* assembly. It is important to recognize, however, that without a reliable method of ordering the contigs, it was not possible to identify larger scale rearrangement events. In fact, ordering of *A. tuberculatus* contigs based on linkage mapping revealed additional rearrangements (fig. 1). Because synteny does not appear perfectly conserved within the *Amaranthus* genus, alternative scaffolding approaches should be implemented to finish the *A. tuberculatus* genome. Conversely, with the contiguity offered via chromatin contact mapping data obtained for *A. palmeri*, several large-scale inverted and translocated regions were seen relative to *A. hypochondriacus*. Additionally, the fragmentation of the chromosome 7 homolog in *A. palmeri* might be attributed to the previous observation that *A. palmeri* contains an additional pair of

chromosomes compared with the other *Amaranthus* species included in this study (Grant 1959). Ultimately, these genomic resources will serve as valuable tools for genomic studies within these species to understand an array of biological questions, with their weediness attributes of particular interest.

Supplementary Material

Supplementary data are available at *Genome Biology and Evolution* online.

Acknowledgments

This work was supported by the USDA National Institute of Food and Agriculture (AFRI project 2018-67013-27818) (J.S.M., D.G., B.P.M., and P.J.T.), the International Max Planck Research School “From Molecules to Organisms” (B.W.), and the Max Planck Society (D.W.).

Literature Cited

- Broman KW, Wu H, Sen S, Churchill GA. 2003. R/qtl: QTL mapping in experimental crosses. *Bioinformatics* 19(7):889–890.
- Browning SR, Browning BL. 2007. Rapid and Accurate Haplotype Phasing and Missing-Data Inference for Whole-Genome Association Studies By Use of Localized Haplotype Clustering. *Am J Hum Genet.* 81(5):1084–1097.
- Camacho C, et al. 2009. BLAST+: architecture and applications. *BMC Bioinformatics* 10(1):421.
- Chin CS, et al. 2013. Nonhybrid, finished microbial genome assemblies from long-read SMRT sequencing data. *Nat Methods.* 10(6):563–569.
- Culpepper AS, et al. 2006. Glyphosate-resistant Palmer amaranth (*Amaranthus palmeri*) confirmed in Georgia. *Weed Sci.* 54(4):620–626.
- English AC, et al. 2012. Mind the gap: upgrading genomes with Pacific Biosciences RS long-read sequencing technology. *PLoS One* 7(11):e47768.
- Gaines TA, et al. 2012. Interspecific hybridization transfers a previously unknown glyphosate resistance mechanism in *Amaranthus* species. *Evol Appl.* 5(1):29–38.
- Grant WF. 1959. Cytogenetic studies in *Amaranthus* I. cytological aspects of sex determination in dioecious species. *Can J Bot.* 37(3):413–417.
- Haas BJ, et al. 2008. Automated eukaryotic gene structure annotation using EVIDENCEModeler and the program to assemble spliced alignments. *Genome Biol.* 9(1):R7.
- Haug-Baltzell A, Stephens SA, Davey S, Scheidegger CE, Lyons E. 2017. SynMap2 and SynMap3D: web-based whole-genome synteny browsers. *Bioinformatics* 33(14):2197–2198.
- Huang S, Kang M, Xu A. 2017. HaploMerger2: rebuilding both haploid sub-assemblies from high-heterozygosity diploid genome assembly. *Bioinformatics* 33(16):2577–2579.
- Humann JL, Lee T, Ficklin S, Main D. 2019. Structural and functional annotation of eukaryotic genomes with GenSAS. In: Kollmar M, editor. *Gene prediction: methods and protocols*. New York: Humana Press. p. 29–51.
- Kim C, et al. 2019. Long-read sequencing reveals intra-species tolerance of substantial structural variations and new subtelomere formation in *C. elegans*. *Genome Res.* 29(6):1023–1035.
- Koren S, et al. 2017. Canu: scalable and accurate long-read assembly via adaptive k-mer weighting and repeat separation. *Genome Res.* 27(5):722–736.
- Koren S, et al. 2018. *De novo* assembly of haplotype-resolved genomes with trio binning. *Nat Biotechnol.* 36(12):1174–1182.
- Korte A, Farlow A. 2013. The advantages and limitations of trait analysis with GWAS: a review. *Plant Methods* 9(1):29.
- Kreiner JM, et al. 2019. Multiple modes of convergent adaptation in the spread of glyphosate-resistant *Amaranthus tuberculatus*. *Proc Natl Acad Sci U S A.* 116(42):21076–21084.
- Laforest M, et al. 2020. A chromosome-scale draft sequence of the Canada fleabane genome. *Pest Manag Sci.* 76(6):2158–2169.
- Lamb JC, Birchler JA. 2003. The role of DNA sequence in centromere formation. *Genome Biol.* 4(5):214.
- Li H. 2018. Minimap2: pairwise alignment for nucleotide sequences. *Bioinformatics* 34(18):3094–3100.
- Li H, et al. 2009. The sequence alignment/map (SAM) format and SAMtools. *Bioinformatics* 25(16):2078–2079.
- Lightfoot DJ, et al. 2017. Single-molecule sequencing and Hi-C-based proximity-guided assembly of *Amaranthus hypochondriacus* chromosomes provide insights into genome evolution. *BMC Biol.* 15(1):74.
- Molin W, Patterson EL, Saski CA. 2020. Homogeneity among glyphosate-resistant *Amaranthus palmeri* in geographically distant locations. *bioRxiv.* doi.org/10.1101/2020.05.14.095729.
- Montgomery JS, Sadeque A, Giacomini DA, Brown PJ, Tranel PJ. 2019. Sex-specific markers for waterhemp (*Amaranthus tuberculatus*) and Palmer amaranth (*Amaranthus palmeri*). *Weed Sci.* 67(4):412–418.
- Patterson EL, Saski C, Küpper A, Beffa R, Gaines TA. 2019. Omics potential in herbicide-resistant weed management. *Plants* 8(12):607.
- Patzoldt WL, Tranel PJ. 2007. Multiple ALS mutations confer herbicide resistance in waterhemp (*Amaranthus tuberculatus*). *Weed Sci.* 55(5):421–428.
- Patzoldt WL, Tranel PJ, Hager AG. 2005. A waterhemp (*Amaranthus tuberculatus*) biotype with multiple resistance across three herbicide sites of action. *Weed Sci.* 53(1):30–36.
- Poplin R, et al. 2017. Scaling accurate genetic variant discovery to tens of thousands of samples. *bioRxiv.* 201178. doi: 10.1101/201178
- Putnam NH, et al. 2016. Chromosome-scale shotgun assembly using an in vitro method for long-range linkage. *Genome Res.* 26(3):342–350.
- R Core Team. 2018. R: a language and environment for statistical computing. Vienna (Austria): R Foundation for Statistical Computing. Available from: <https://www.R-project.org/>. Accessed September 2, 2020.
- Ravet K, et al. 2018. The power and potential of genomics in weed biology and management. *Pest Manag Sci.* 74(10):2216–2225.
- Riggins CW, Peng Y, Stewart CN, Tranel PJ. 2010. Characterization of de novo transcriptome for waterhemp (*Amaranthus tuberculatus*) using GS-FLX 454 pyrosequencing and its application for studies of herbicide target-site genes. *Pest Manag Sci.* 66(10):1042–1052.
- Sauer JD. 1957. Recent migration and evolution of the dioecious amaranths. *Evolution* 11(1):11–31.
- Sauer JD. 1967. The grain amaranths and their relatives: a revised taxonomic and geographic survey. *Ann Mo Bot Gard.* 54(2):103–137.
- Smit AFA, Hubley R, Green P. 2013. RepeatMasker Open-4.0. Available from: <http://www.repeatmasker.org>. Accessed September 2, 2020.
- Stanke M, Steinkamp R, Waack S, Morgenstern B. 2004. AUGUSTUS: a web server for gene finding in eukaryotes. *Nucleic Acids Res.* 32(Web Server):W309–W312.
- Stetter MG, Schmid KJ. 2017. Analysis of phylogenetic relationships and genome size evolution of the *Amaranthus* genus using GBS indicates the ancestors of an ancient crop. *Mol Phylogenet Evol.* 109:80–92.
- Tranel PJ, Riggins CW, Bell MS, Hager AG. 2011. Herbicide resistances in *Amaranthus tuberculatus*: a call for new options. *J Agric Food Chem.* 59(11):5808–5812.
- Tranel PJ, Trucco F. 2009. 21st-century weed science: a call for *Amaranthus* genomics. In: Stewart CN Jr, editor. *Weedy and invasive plant genomics*. Ames (IA): Blackwell. p. 53–81
- Truong HT, et al. 2012. Sequence-based genotyping for marker discovery and co-dominant scoring in germplasm and populations. *PLoS One* 7(5):e37565.
- Vincent G, Cappadocia M. 1987. Interspecific hybridization between common ragweed (*Ambrosia artemisiifolia*) and giant ragweed (*A. trifida*). *Weed Sci.* 35(5):633–636.
- Waselkov KE, Boleda AS, Olsen KM. 2018. A phylogeny of the genus *Amaranthus* (Amaranthaceae) based on several low-copy nuclear loci and chloroplast regions. *Syst Bot.* 43(2):439–458.
- Xin Z, Chen J. 2012. A high throughput DNA extraction method with high yield and quality. *Plant Methods* 8(1):26.

Associate editor: Tanja Slotte